

# Thermal modelling and performance assessment of a circular greenhouse with solar chimney assisted ventilation and fog cooling

D. Misra, S. Ghosh\*

(Department of Mechanical Engineering, Indian Institute of Engineering Science and Technology, Shibpur, Howrah-711103, India)

**Abstract:** This paper presented a conceptualized model of a solar chimney-assisted naturally ventilated circular greenhouse applicable for hot and arid regions. Instead of conventional rectangular shape, a circular shape was chosen which made the greenhouse independent of wind direction and orientation with regards to the wind-induced ventilation. Pressurised fogging system was considered as the mode of distributed evaporative cooling. A circular twin-wall solar chimney was centrally mounted which is suitably sized to provide buoyancy-induced natural ventilation. The solar induced ventilation was sufficient, giving 0.6-0.75 air change per minute (ACM). The analysis revealed that during the peak ambient temperatures, the greenhouse inside temperature could be lowered by 4°C to 6°C below the ambient employing an optimized fogging cycle with spray time/interval period of 1.5 min/2 min.

**Keywords:** greenhouse, solar chimney, ventilation, evaporative cooling, fogging cycle

**Citation:** Misra, D., and S. Ghosh. 2018. Thermal modelling and performance assessment of a circular greenhouse with solar chimney assisted ventilation and fog cooling. *Agricultural Engineering International: CIGR Journal*, 20(4): 108–118.

## 1 Introduction

Greenhouses in hot and humid regions suffered from excessive temperature during sunshine period, as solar radiation intensity is very high. The reductions of temperature well below the ambient temperature as well as sufficient ventilation are necessary for effective plant growth. In general, fan ventilated greenhouses usually employ a wetted pad at one end of an enclosed space to control the greenhouse temperature rise, whereas in naturally ventilated system fogging or misting system is usually employed. Fan ventilated greenhouses require lots of grid power while naturally ventilated greenhouses suffer from poor ventilation rate. Thus, the development of non-traditional and energy efficient greenhouse is a need for sustainable and protected cultivation providing both cooling and ventilation.

During the last two decades, extensive work has been done on greenhouse ventilation and evaporative cooling systems. Many studies have been conducted on fan-pad ventilation system. Ganguly and Ghosh (2007), Bartzanas and Kittas (2005) studied fan and pad ventilation system to predict greenhouse temperature and found that air temperature near the pad end was well below the ambient. However, there is a large temperature variation along the length of the greenhouse. Ganguly et al. (2010), Al-Heelal et al. (2006) carried out a study on solar photovoltaic power system to meet the power requirement of fan-pad greenhouse system. Misra and Ghosh (2013) proposed a distributed evaporative cooling greenhouse equipped with pads on side walls and fans on roof. They presented a thermal model to predict the inner temperatures considering energy balance of the greenhouse components. Again, Misra and Ghosh (2017a) conducted a performance study to predict the greenhouse air temperature under dual ventilation mode and with external evaporative cooling. Many researchers proposed theoretical models to predict ventilation rate of naturally ventilated greenhouse such as Kittas et al. (1997), Teitel and Tanny (1999), Boulard and Bailey (1993), Ganguly

**Received date:** 2017-10-26    **Accepted date:** 2018-02-11

\*Corresponding author: Ghosh, S., Department of Mechanical Engineering, Indian Institute of Engineering Science and Technology, Shibpur, Howrah-711103, India. Phone: +91-33-26684561. Fax: +91-33-26682916. Email: [sudipghosh.becollege@gmail.com](mailto:sudipghosh.becollege@gmail.com).

and Ghosh (2009), etc. They conducted their study on naturally ventilated greenhouse and identified that the position of roof ventilation, wind speed, effective height of the air column were the key factors affecting the natural ventilation rate. Boulard and Baille (1993), Arbel et al. (1999), Abdel-Ghany et al. (2006), Mirja et al. (2016), Misra and Ghosh (2017b), and others developed the fog evaporative cooling models for naturally ventilated greenhouses to investigate the fogging effect on greenhouse air temperature. However, the effect of solar chimney has not been studied for greenhouse ventilation. Although solar chimney based power generation system has been developed and such plants are currently in existence (Ali, 2017; Hussain and Ogboo, (2016); Panse et al., 2011; Koonsrisuk and Chitsomboon 2013; etc.). The solar chimneys and solar stacks have also been modelled and designed in works related to passive ventilation of buildings. Ong (2003) presented an analytical model to predict solar chimney performance for room ventilation. He had considered glass covered chimney with rectangular black absorber plate of 2 m height fitted on one of the side walls of a room. Again, Ong and Chow (2003) presented an experimental study on a solar chimney of the same height as presented earlier, only changing inlet and outlet opening width. Bansal et al. (2005) presented and experimentally validated a thermal model for a small size window type solar chimney for predicting the temperature and air velocity. They found a good match between the theoretical prediction and experimental values. Mathur et al. (2006) experimented on a 1 m high solar chimney-assisted room ventilation system. They found that the maximum ventilation rate was of 5.6 air change per hour (ACH) for the 27 m<sup>3</sup> room, when the solar radiation intensity was 700 W m<sup>-2</sup>. Burek and Habeb (2007) experimented on a test rig equivalent to a small vertical solar chimney (area 0.948 m<sup>2</sup>), which was made of a vertical absorber and transparent cover to form an air flow channel. From the experimental observation they developed correlations of ventilation rate of air and thermal efficiency. Bassiouny and Koura (2008) carried out numerical study related to solar chimney-assisted room ventilation to investigate the effect of inlet air channel width as well as air flow characteristics. It was found that increasing the chimney

inlet width by three times, air change per hour (ACH) was increased nearly 11%. They had found correlations of absorber mean temperature and exit air velocity both were varied with solar radiation intensity. Tan and Wong (2013) had conducted a study for a tropical building to observe the solar chimney performance as well as to optimize the chimney design. Saleem et al. (2016) studied solar chimney assisted room ventilation to achieve optimum ventilation rate. There are instances of using solar chimneys for others specific purposes. For example, a 10 m polycarbonate solar chimney has been built in a study reported by Zaragoza et al. (2007) for solar distillation and water collection. Bello et al. (2015) built a glass stack with triangular absorber fitted inside for wood drying.

A survey of literature thus reveals that incorporating a solar chimney in a greenhouse could enhance its natural ventilation owing to stack effect. It could be argued that the evaporative cooling together with solar chimney ventilation would provide a better cooling effect for a greenhouse. In a conventional naturally ventilated greenhouse, air flows through the vent openings as a pressure difference occurs because of the temperature variation between the inside and the outside air as well as the wind velocity. The pressure difference of air increases when the central distance between vents (height of air column inside the greenhouse) becomes more. Thus, air flow rate of a naturally ventilated greenhouse depends on the height of the greenhouse. However, greenhouse can be made up to a certain height only. Thus, instead of increasing greenhouse height, a solar chimney can be fitted at the roof to ensure more air exchange.

The present paper describes such a greenhouse with a double wall circular solar chimney. The greenhouse is considered as circular in shape. Being circular, this system is independent of wind direction and orientation, which are the major factors affecting a naturally ventilated greenhouse. A double wall construction of the chimney is expected to enhance the ventilation performance. The circular chimney is mounted centrally to predict the ventilation rate as well as the cooling performance of the greenhouse. Internal shading and intermittent fog cooling are considered to control the greenhouse temperature. A thermal model, based on

energy interaction has been developed.

## 2 General arrangement of the proposed greenhouse

General arrangement of the greenhouse and details of its different components are shown in Figure 1. The diameter of the circular covered area is 12 m and the central canopy height is 4 m. A long cylindrical double-wall chimney, 10 m long, is extended from the central part of the canopy. The elevation and the plan of the greenhouse are shown in Figure 1(a) and Figure 1(b), respectively. Parts 'A' and 'C' indicate parts of the vertical wall covered by polyethylene, while 'B' is space that remains open or is covered with insect screen. Section 'B', which is 1.5 m height, is responsible for air flow from outside into the greenhouse. Thus, the wind can freely flow in, from any direction and assists in ventilation. The greenhouse air is allowed to pass through the inner cylindrical channel of the chimney (part 'E').

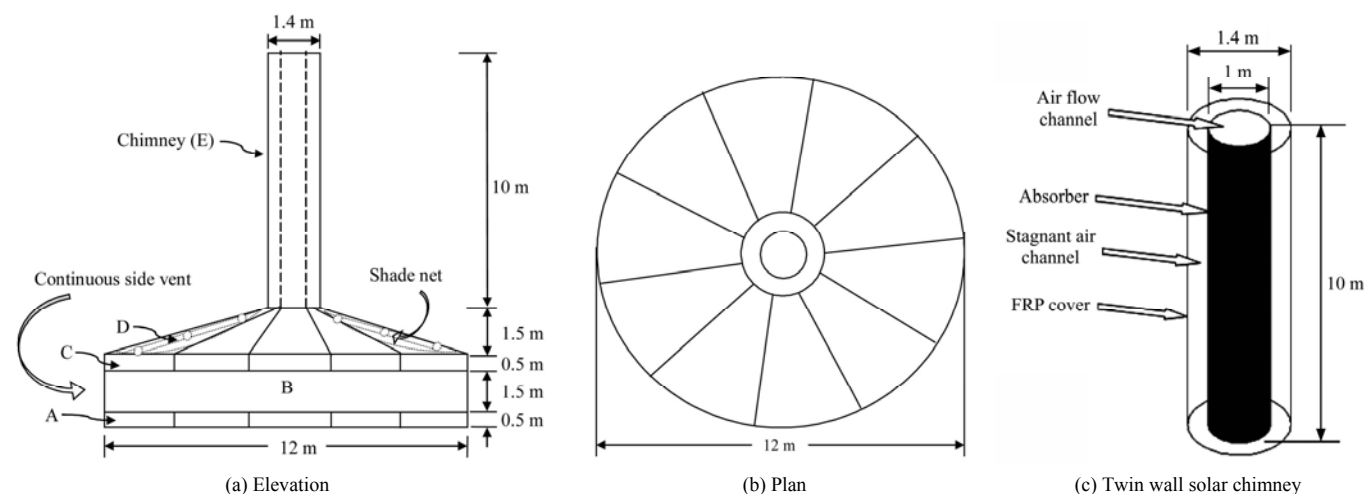


Figure 1 General arrangement and dimensional details of the greenhouse

## 3 Thermal modelling

To model the heat interactions and the air flow characteristics of the solar chimney, some simplifying assumptions are considered, which are as follows:

- (i) The temperature distribution is uniform for the outer and inner walls of the chimney.
- (ii) One-dimensional heat transfer equations have been considered.
- (iii) The inlet air temperature of the solar chimney is considered to be the greenhouse air temperature.
- (iv) Resistance to the air flow is not taken into account.

Shade nets are aligned with the canopy, inside the greenhouse, to check the excess solar radiation. During summer 75% shade net is placed beneath the canopy walls and during winter 50% shade net is used. The chimney is formed by two concentric thin walls, as shown in Figure 1(c): the outer wall is built of transparent fibre reinforced plastic (FRP) and the inner wall is built of blackened aluminium so as to act as absorber of solar heat. The outer wall mean diameter is 1.4 m and the inner wall mean diameter is 1.0 m. There is stagnant air between two concentric cylinders, as it is properly sealed. The ends are covered by FRP between the FRP and absorber wall. The blackened aluminium absorber wall heats up the greenhouse air exiting through the chimney. The canopy (portion 'D') is made of FRP. The greenhouse is equipped with fogging system to cool the inside air by evaporative cooling. Four-way foggers are uniformly distributed throughout the greenhouse under the shed net.

(v) Air inside the chimney is assumed to be a non-radiating heat absorbing fluid.

(vi) Only circumferential heat loss from the chimney is considered

(vii) The air in the annular gap (between absorber wall and outer cover) of the chimney is confined and stagnant.

(viii) Neglecting heat absorption of the other greenhouse constructional elements.

### 3.1 Energy balance equation of greenhouse air

Simplified energy balance equation for an instance of the greenhouse air can be written as (in the same line as

Misra and Ghosh (2017b)):

$$m_{gh} C_p \frac{dT_{gh}}{dt} = Q_i - h_c A_c (T_{gh} - T_a) - m_v C_p (T_{fa} - T_{gh}) - \lambda \beta m_{fog} - \lambda A_f LAI \kappa (e_p - e_{gh}) \quad (1)$$

where,  $m_{gh}$  is the mass of the greenhouse air;  $C_p$  is the specific heat of greenhouse air;  $T_{gh}$  is the temperature of the greenhouse air;  $A_c$  is the area of canopy cover and side walls;  $Q_i$  is the sensible heat gain of greenhouse air;  $h_c$  is the heat transfer coefficient of greenhouse cover;  $T_a$  is the temperature of the ambient air;  $m_v$  is the mass flow rate of the ventilated air;  $T_{fa}$  is the mean temperature of air in the solar chimney;  $\lambda$  is the latent heat of evaporation;  $\beta$  is the fog evaporation factor;  $m_{fog}$  is the mass of supplied water by fog nozzles;  $A_f$  is the area of floor;  $e_{ps}$  is the saturated vapour pressure corresponding to plant temperature and  $e_a$  is the water vapour pressure corresponding to the greenhouse temperature;  $\kappa$  is the stomatal boundary layer conductance. Leaf area index (LAI) is defined as the ratio of cumulative one-sided area of leaf tissue to the ground area of the greenhouse (Bréda, 2003). LAI value depends on plant species and plant canopy structure (Sampson, and Allen, 1995). For young plants it is considered to be 0.25 (Abdel-Ghany et al., 2006) and the same is assumed in the present study.

The first part of the right hand side of the Equation (1) represents net radiant heat gain by the greenhouse air ( $Q_i$ ), given by

$$Q_i = A_{pa} I \tau \alpha (1 - SF) \quad (2)$$

where,  $I$  is the normal solar radiation intensity ( $W m^{-2}$ );  $\tau$  is the transmissivity of greenhouse cover;  $\alpha$  is the absorptivity of the greenhouse (overall absorptivity specifying the fraction of net solar heat gain);  $A_{pa}$  is the projected area of the greenhouse;  $SF$  is the shading factor of the shade net (defined as the fraction of incoming radiation obstructed by the shade net, placed beneath the canopy covering). A shading factor of 0.75 is considered during the summer and a factor of 0.5 is considered during winter. Additional shading due to the solar chimney absorber (blackened cylindrical wall) is negligible (less than 5% of the canopy area will have full shade as against applied shade net of 75% or 50%).

In the Equation (1), the second part of the right hand side indicates convective heat exchange between greenhouse and ambient air, the third part represents

energy exchange due to ventilation of greenhouse air, the fourth part indicates latent heat exchange by the fog water evaporation and the fifth part represents heat exchange by the crop transpiration.

The latent heat of vaporization of water  $\lambda$  ( $J kg^{-1}$ ) of Equation (1) is given by Smolík et al. (2001)

$$\lambda = 10^3 \times (3.4702 \times 10^3 - 5.7352 \times T + 1.1687 \times 10^{-2} T^2 - 1.3478 \times 10^{-5} T^3) \quad (3)$$

where,  $T$  is the temperature in K.

Solution of the Equation (1) requires a set of input parameters (for a defined fogging cycle), which are shown in Table 1. The Equation also needs an initial value of mass flow rate of the air. In the present greenhouse system, mass flow rate occurs due to variation of the solar chimney air temperature against ambient temperature as well as wind effects. An expression for mass flow rate of air through the chimney was suggested by Bansal et al. (2005) and Andersen (1995) considering only the thermal buoyancy effect. Ganguly and Ghosh (2009), in their naturally ventilated greenhouse model, considered both thermal buoyancy and wind effects. The total mass flow rate through the solar chimney greenhouse, along with the same line considering the effect of height of the greenhouse and chimney height can be expressed as:

$$m_v = \rho_{fa} C_d \left[ \left( \frac{A_{sv} A_{ci}}{\sqrt{A_{sv}^2 + A_{ci}^2}} \right) \left( \sqrt{2g \frac{T_{fa} - T_a}{T_a} (H_{gh} + H_{ch})} \right) + \left( \frac{A_{sv} + A_{ci}}{2} \right) (C_w v_w) \right] \quad (4)$$

where,  $\rho_{fa}$  is the density of air;  $A_{sv}$  is the side vent area;  $A_{ci}$  is the inside area of solar chimney;  $H_{gh}$  is the vertical distance between the midpoints of the side and bottom of the chimney;  $H_{ch}$  is the height of chimney;  $C_d$  and  $C_w$  are the discharge coefficient and wind effect coefficient, respectively;  $v_w$  is the free wind velocity ( $m s^{-1}$ ). When chimney is not considered  $T_{fa}$  is replaced by  $T_{gh}$ .

In order to compute the mass flow rate of air, where solar chimney is being used, the air temperature of the solar chimney must be calculated. This can be done by computing the temperatures for the various sections through the energy balances for the chimney cover, stagnant air, absorber wall and the flowing air through the chimney.

### 3.2 Energy balance equation of solar chimney

Heat interaction, occurred in the solar chimney components, mainly chimney cover, stagnant air, absorber wall and the flowing air into the chimney. Figure 2 shows heat interactions occurring through solar chimney components.

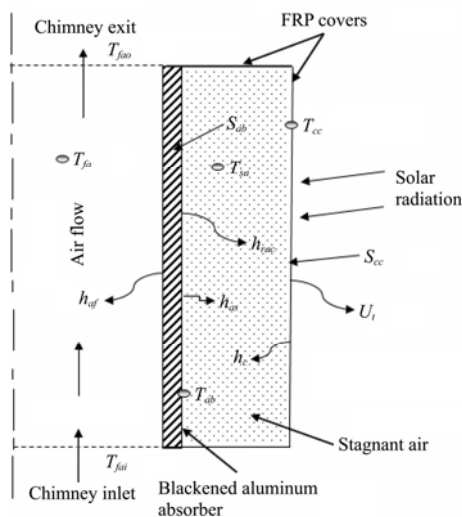


Figure 2 Sectional view of solar chimney showing heat interaction

#### 3.2.1 Energy balance equation of solar chimney cover

$$S_{cc}A_{cc} + h_{rac}A_{ab}(T_{ab} - T_{cc}) = h_c A_{cc}(T_{cc} - T_{sa}) + U_t A_{cc}(T_{cc} - T_a) \quad (5)$$

where,  $S_{cc}$  is the radiant flux of chimney cover ( $\text{W m}^{-2}$ );  $A_{cc}$  is area of chimney cover;  $h_{rac}$  is the heat transfer coefficient between absorber wall ( $\text{W m}^{-2} \text{K}^{-1}$ ) and chimney cover;  $A_{ab}$  is the area of absorber wall ( $\text{m}^2$ );  $T_{ab}$  is the temperature of the absorber wall;  $T_{cc}$  is the temperature of chimney cover (K);  $h_c$  is the heat transfer coefficient between cover and stagnant air ( $\text{W m}^2 \text{K}^{-1}$ );  $T_{sa}$  is the temperature of stagnant air (K);  $U_t$  is the overall top loss coefficient ( $\text{W m}^2 \text{K}^{-1}$ ).

In the Equation 5, the first part of the left hand side indicates radiant heat absorbed by FRP cover of the solar chimney and the second part of the left hand side indicates radiant heat coming from the aluminium absorber wall. The first part of the right hand side indicates convective heat transfer from FRP cover to stagnant air and the second part indicates overall heat transfer from outer FRP chimney cover to ambient air.

Radiation heat flux absorbed by the chimney cover ( $S_{cc}$ ) is given by

$$S_{cc} = \alpha_{cc} I \quad (6)$$

where,  $\alpha_{cc}$  is the absorptivity of chimney cover;  $I$  is the solar radiation intensity ( $\text{W m}^{-2}$ ).

The radiative heat transfer coefficient ( $h_{rab}$ ) can be expressed as (Ong, 2003):

$$h_{rac} = \sigma(T_{cc}^2 + T_{ab}^2)(T_{cc} + T_{ab}) / (1/\epsilon_{cc} + 1/\epsilon_{ab} - 1) \quad (7)$$

where,  $\sigma$  is the Stefan Boltzmann constant;  $\epsilon_{cc}$  is the emissivity of chimney cover;  $\epsilon_{ab}$  is the emissivity of aluminium absorber.

The overall heat loss coefficient ( $U_t$ ) can be expressed as the summation of convective heat transfer coefficient due to wind ( $h_{fw}$ ), radiative heat transfer coefficient between the FRP chimney cover and the sky ( $h_{rcs}$ ) and conductive coefficient of FRP cover ( $h_{cc}$ ), written as (Bansal et al., 2005; Mathur et al., 2006):

$$U_t = h_w + h_{rcs} + h_c \quad (8)$$

The heat transfer coefficient caused by wind ( $h_w$ ) is written as (Ong and Chow, 2003):

$$h_w = 5.7 + 3.8v_w \quad (9)$$

The radiative heat transfer coefficient ( $h_{rcs}$ ) between the chimney cover and the sky is given by (Ong and Chow, 2003)

$$h_{rcs} = \sigma \epsilon_{cc} (T_{cc} + T_{sky})(T_{cc}^2 + T_{sky}^2)(T_{cc} - T_{sky}) / (T_{cc} - T_a) \quad (10)$$

The sky temperature ( $T_{sky}$ ) is expressed as (Swinbank, 1963):

$$T_{sky} = 0.0552T_a^{1.5} \quad (11)$$

#### 3.2.2 Energy balance equation of stagnant air

$$h_{as}A_{ab}(T_{ab} - T_{sa}) + h_c A_{cc}(T_{cc} - T_{sa}) = m_{sa} C_p (T_{sa} - T_a) \quad (12)$$

where,  $h_{as}$  is the heat transfer coefficient between the absorber and the stagnant air;  $m_{sa}$  is the mass of stagnant air;  $T_{sa}$  is the temperature of the stagnant air.

In the Equation (12), the first part of the left hand side indicates convective heat transfer from absorber wall to stagnant air, the second part represents convective heat transfer from chimney cover to stagnant air. The right hand side represents heat gain by stagnant air.

#### 3.2.3 Energy balance equation of absorber wall

$$S_{ab}A_{ab} = h_{af}A_{ab}(T_{ab} - T_{fa}) + h_{as}A_{ab}(T_{ab} - T_{sa}) + h_{rac}A_{ab}(T_{ab} - T_{cc}) \quad (13)$$

where,  $S_{ab}$  is the radiant heat flux by the absorber;  $h_{af}$  is the heat transfer coefficient between the absorber wall and flowing air;  $T_{fa}$  is the temperature of flowing air inside the chimney.

In the Equation (13), left hand side indicates radiant heat gain by the aluminium absorber wall. The first part of the right hand side indicates convective heat transfer from chimney cover to flowing air, the second part indicates convective heat transfer to stagnant air and the third part indicates radiant heat transfer from the absorber wall to the FRP chimney cover.

Solar energy gained by the aluminium absorber wall ( $S_{ab}$ ) is given by

$$S_{ab} = \alpha_{ab} \tau I \quad (14)$$

where,  $\alpha_{ab}$  is the absorptivity of the absorber;  $\tau$  is the transmissivity of FRP chimney cover.

3.2.4 Energy balance equation of flowing air stream of the chimney

$$h_{af} A_{ab} (T_{ab} - T_{fa}) = m_v C_p (T_{fao} - T_{fai}) \quad (15)$$

where,  $T_{fao}$  is the temperature of flowing air outlet to the chimney;  $T_{fai}$  is the temperature of flowing air inlet to the chimney.

In the Equation (15), left hand side indicates convective heat transfer from absorber to the flowing air stream of the chimney; right hand side represents useful heat gain of the flowing air stream.

The heat transfer co-efficient of the flowing air stream can be written as (Incropera and Dewitt, 2006):

$$h_{af} = \frac{Nu k_{fa}}{d_{cc}} \quad (16)$$

Mean air temperature of fluid is given by

$$T_{fa} = \gamma T_{fao} + (1 - \gamma) T_{fai} \quad (17)$$

where,  $\gamma$  represents the mean temperature approximation coefficient and its value is taken as 0.74 (Ong and Chow, 2003).

### 3.3 Properties of air

Following property relations were used (all expressed as functions of temperature,  $T$ ), which were evaluated at the respective mean temperatures (Incropera and Dewitt, 2006).

Co-efficient of volumetric expansion

$$\Delta = 1/T \quad (18)$$

Air viscosity

$$\mu_{fa} = [1.846 + 0.00472(T - 300)] \times 10^{-5} \quad (19)$$

Air density

$$\rho_{fa} = [1.1614 - 0.00353(T - 300)] \quad (20)$$

Air heat conductivity

$$k_{fa} = [0.0263 + 0.000074(T - 300)] \quad (21)$$

Air specific heat

$$C_p = [1.007 + 0.00004(T - 300)] \times 10^3 \quad (22)$$

The average heat transfer coefficient for air under natural convection is evaluated considering the following equation, as Incropera and Dewitt (2006):

When flow is laminar ( $Ra < 10^9$ )

$$Nu = (0.68 + 0.67 Ra^{\frac{1}{4}}) / [1 + (0.492 / Pr)^{\frac{9}{16}}]^{\frac{4}{9}} \quad (23)$$

When flow is turbulent ( $Ra > 10^9$ )

$$Nu = \left\{ (0.825 + 0.38 Ra^{\frac{1}{6}}) / \left\{ 1 + (0.492 / Pr)^{\frac{9}{16}} \right\}^{\frac{8}{27}} \right\}^2 \quad (24)$$

## 4 Solution procedure

The five energy balance equations Equation (1), Equation (5), Equation (12), Equation (13) and Equation (15) and a mass flow rate equation (Equation (4)), are to be solved for six unknown variables ( $T_{cc}$ ,  $T_{sa}$ ,  $T_{ab}$ ,  $T_{fa}$ ,  $T_{gh}$ , and  $m_v$ ). In solving these equations other parameters (heat transfer coefficients, absorbed radiant energies etc) are calculated from their relevant equations as stated above. The model equations as described above are integrated in programme code using F-Chart Software (Engineering Equation Solver). The solution scheme is described in the flow chart shown in Figure 3. An initial guess is made for  $T_{fa}$  and  $T_{gh}$ ; accordingly, first estimate of  $m_v$  and  $T_{gh}$  are made using Equation (1) and Equation (5). Then other

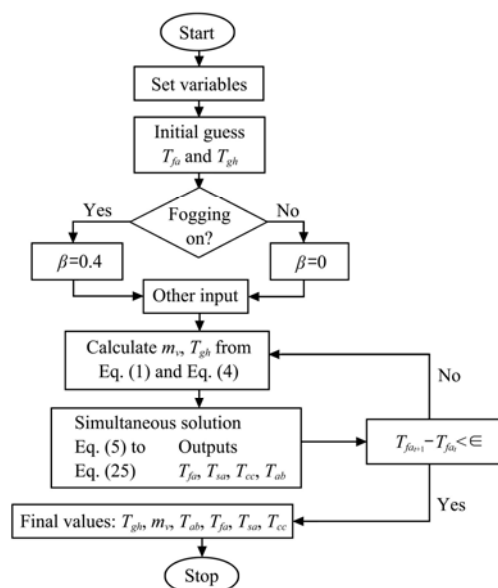


Figure 3 Flow chart for computation procedure

four equations are solved simultaneously for the other unknowns. The calculation loop is repeated until the temperature parameters are stabilized. Temperature of the ambient air and solar radiation intensities are taken from the book of Tiwari (2002) for the climatic data of Kolkata (22°34'N, 88°24'E), India.

**Table 1 Model input parameters**

| Parameters   | Values  |
|--|---|
| Greenhouse covering area ( $A_{gc}$ )                  | 173 m <sup>2</sup>  |
| Area of greenhouse floor ( $A_f$ )                     | 113.14 m <sup>2</sup>   |
| Area of chimney cover ( $A_{cc}$ )                     | 1.538 m <sup>2</sup>  |
| Inner area of chimney ( $A_{ci}$ )                     | 0.785 m <sup>2</sup>  |
| Area of side vent ( $A_{sv}$ )                         | 56.54 m <sup>2</sup>  |
| Leaf area index ( $LAI$ )                              | 0.25 (Abdel-Ghany et al., 2006)   |
| Coefficient of discharge ( $C_d$ )                     | 0.6 (Boulard et al., 1999)  |
| Wind coefficient ( $C_w$ )                             | 0.14 (Boulard et al., 1999)   |
| Greenhouse volume ( $G_{vol}$ )                        | 349 m <sup>3</sup>  |
| Heat transfer coefficient of chimney cover ( $h_c$ )   | 4.5 W m <sup>-2</sup> K <sup>-1</sup><br>(Ganguly and Ghosh, 2007)                    |
| Heat transfer coefficient of stagnant air ( $h_{as}$ ) | 10 W m <sup>-2</sup> K <sup>-1</sup><br>(Incropera and Dewitt, 2006)                  |
| Free wind velocity ( $v_w$ )                           | 1.0 m s <sup>-1</sup> (Ganguly and Ghosh, 2009)                                       |
| Emissivity of chimney cover ( $\epsilon_{cc}$ )        | 0.94 (Rachmat and Horibe, 1999)   |
| Emissivity of absorber ( $\epsilon_{ab}$ )             | 0.95 (Ong and Chow, 2003)   |
| Absorptivity of chimney cover ( $\alpha_{cc}$ )        | 0.07 (Rachmat and Horibe, 1999)   |
| Absorptivity of absorber ( $\alpha_{ab}$ )             | 0.95 (Ong and Chow, 2003)   |
| Transmissivity of chimney cover ( $\tau$ )             | 0.78 (Ganguly and Ghosh, 2007)  |
| Fog evaporation factor ( $\beta$ )                     | 0.4 (Misra and Ghosh, 2017b)  |
| Mass of spraying water ( $m_{fog}$ )                   | $0.175 \times 10^{-3}$ kg m <sup>-2</sup> s <sup>-1</sup><br>(Misra and Ghosh, 2017b) |

## 5 Results and discussion

Table 2 shows the base case performance of the solar

**Table 2 Base case performance for different representative days of Kolkata with a fogging cycle (1.5-2 min) during peak ambient temperatures**

| Parameters<br>(fogging cycle 1.5 min on,<br>2 min off)        | Summer (May), RH=0.5,<br>Ta=35.8°C, SF=0.75,<br>I=762 W m <sup>-2</sup> | Monsoon (August), RH=0.6,<br>Ta=32°C, SF=0.75,<br>I=727 W m <sup>-2</sup> | Spring (March), RH=0.5,<br>Ta=34.3°C, SF = 0.75,<br>I=653 W m <sup>-2</sup> | Winter (January), RH=0.5,<br>Ta=26.8°C, SF=0.50,<br>I=490 W m <sup>-2</sup> |
|---|---|---|---|---|
| Stabilized fogging cycle average<br>temperature ( $T_{ghs}$ ) | 29.96   | 27.26   | 28.41   | 23.82   |
| ACM   | 0.65 - 0.75   | 0.60 - 0.70   | 0.62 - 0.72   | 0.60 - 0.64   |

Figure 4 presents how consecutive fogging cycles influence the greenhouse air temperature. Four representative days, one each for summer, monsoon, winter and spring, have been considered. Spraying of fog water reduces the greenhouse temperature, while interval periods increase the air temperature owing to solar heat gain. It is seen that the stable temperature cycle is obtained after four to five consecutive fogging cycles as

thereafter fogging does not lower the air temperature significantly. Fogging cycle average greenhouse temperature ( $T_{ghs}$ ) can be computed from the plot under stabilized condition, as shown in each of the plots. Two most influencing factors affecting the ventilation rate are solar radiation intensity and height of the chimney. The ventilation performance of the greenhouse is therefore analyzed by varying these two parameters.

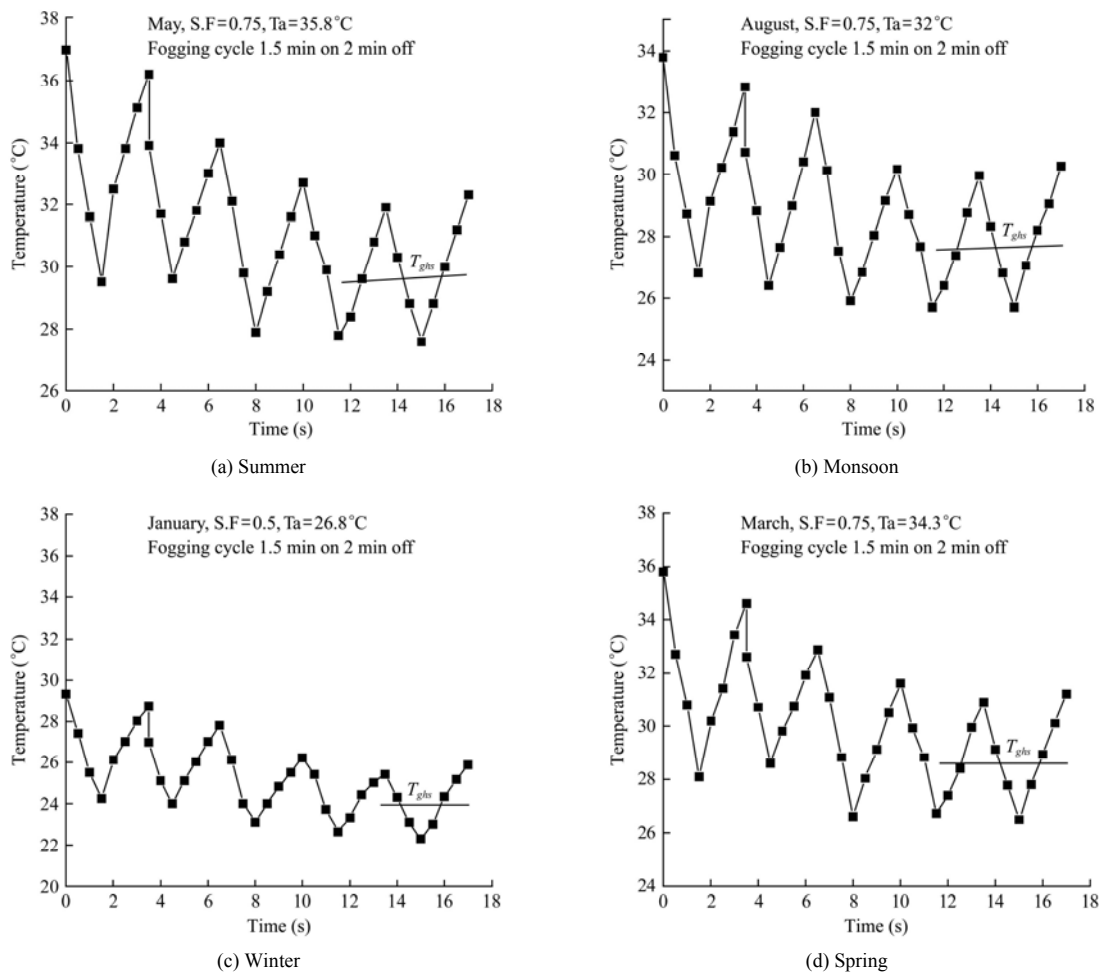


Figure 4 Temperature profiles of greenhouse air for various representative days of the months

Figure 5 shows the effect of solar insolation on ventilation rate through the greenhouse for a fixed ambient temperature of 30°C. To different shade factors, typical of summer ( $SF=0.75$ ) and winter ( $SF=0.5$ ) are considered. It is observed, as expected, that higher solar insolation level also results in higher ventilation rate. It is also observed that higher shading factor reduces ventilation rate.

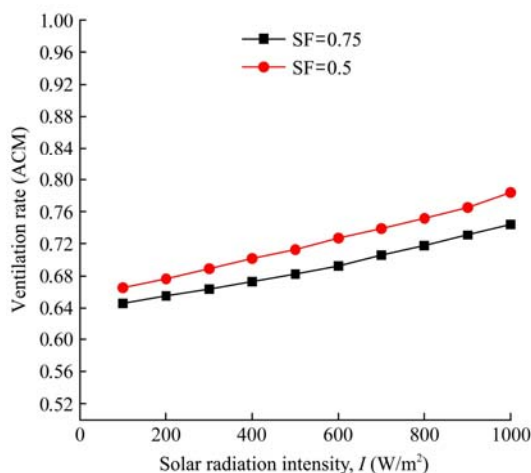


Figure 5 Effect of solar radiation intensity on ventilation rate

Figure 6 shows variation of greenhouse ventilation rate with chimney height. Two sets of climatic parameters, representing typical summer and winter conditions, are considered. It is seen that the ventilation rate increases almost linearly with chimney height. It is further seen that higher ventilation rate occurs in summer than that in winter for a given chimney height, which is due to higher solar heat gain by the chimney absorber.

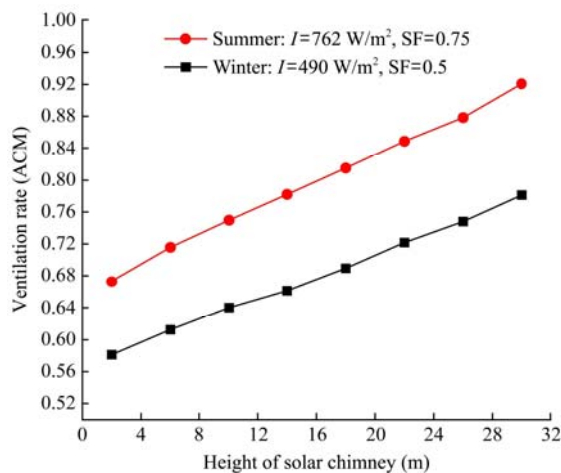


Figure 6 Effect of solar chimney height on ventilation rate



Figure 7 shows the effect of solar radiation intensity on solar chimney parameters like chimney FRP cover temperature, absorber wall temperature and the mean air temperature of the solar chimney. It is found that the absorber wall temperature increases rapidly with increase in solar radiation intensity. However, the mean air temperature increases only slightly with increase in solar radiation, as the air flow rate also increases. Canopy shading does not significantly effects the chimney parameters, excepting the air mass flow rate.

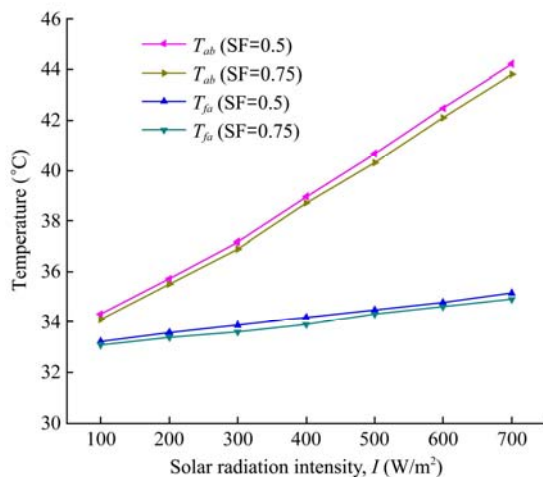


Figure 7 Effect of solar radiation intensity on solar chimney temperatures for  $T_a=30^{\circ}C$

## 6 Conclusion

A conceptualized model has been presented in this paper for a circular greenhouse equipped with a double-wall solar chimney and fogging system. The model is based on the energy balance equations under steady state of the solar chimney, and it predicts the ventilation rate as well as air temperature inside the greenhouse. The results suggest that the solar chimney improves the ventilation rate considerably when compared with other natural ventilation greenhouses. It is also found that greenhouse predicted temperatures lie between  $4^{\circ}C$ - $6^{\circ}C$  below the ambient temperature considering a fogging cycle of 1.5 min spraying time with 2 min interval period when ambient conditions are hot and dry. It is observed that chimney height is the important parameter to improve the ventilation rate. The greenhouse performance can be influenced by solar radiation intensity and height of the solar chimney significantly.

## Nomenclature

|           |   |
|-----------|---|
| $A$       | area ( $m^2$ )  |
| ACM       | air change per min  |
| $C_p$     | specific heat ( $J\ kg^{-1}\ m^{-1}\ K^{-1}$ )            |
| $h$       | heat transfer coefficient ( $W\ m^{-2}\ K^{-1}$ )         |
| $U_t$     | overall heat transfer coefficient ( $W\ m^{-2}\ K^{-1}$ ) |
| $I$       | solar radiation intensity ( $W\ m^{-2}$ )                 |
| $S$       | radiant heat flux ( $W\ m^{-2}$ )                         |
| $T$       | temperature (K)   |
| $K$       | thermal conductivity ( $W\ m^{-1}\ K^{-1}$ )              |
| $H$       | height (m)  |
| $m$       | mass (Kg or $Kg\ s^{-1}$ )                                |
| $d$       | diameter (m)  |
| $v$       | velocity ( $m\ s^{-1}$ )                                  |
| $G_{vol}$ | volume of greenhouse air ( $m^3$ )                        |
| $C_d$     | discharge co-efficient                                    |
| $C_w$     | wind co-efficient   |
| $\kappa$  | stomatal boundary layer conductance ( $Wm^{-1}K^{-1}$ )   |
| $e$       | vapour pressure (kPa)                                     |

## Abbreviations

|       |   |
|-------|---|
| $ab$  | absorber                                      |
| $af$  | absorber to flowing fluid                     |
| $c$   | cover   |
| $ca$  | cover to air                                  |
| $cc$  | chimney cover                                 |
| $ch$  | chimney                                       |
| $ci$  | chimney inner cross section                   |
| $d$   | diffuse                                       |
| $f$   | floor   |
| $fa$  | flowing air                                   |
| $g$   | global  |
| $gh$  | greenhouse                                    |
| $ghs$ | greenhouse stabilized                         |
| $p$   | plant   |
| $rac$ | radiation from absorber wall to chimney cover |
| $rcs$ | radiation from chimney cover to sky           |
| $sa$  | stagnant air                                  |
| $sv$  | side vent                                     |
| $w$   | wind  |
| $v$   | ventilated air                                |

## Greek letters

|               |   |
|---------------|---|
| $\alpha$      | absorptivity  |
| $\beta$       | fraction of fog water evaporation   |
| $\Lambda$     | thermal expansion co-efficient ( $\text{K}^{-1}$ )                                  |
| $\varepsilon$ | emissivity  |
| $\sigma$      | Stefan-Boltzmann constant ( $5.67 \times 10^{-8} \text{ W m}^{-2} \text{ K}^{-4}$ ) |
| $\tau$        | transmissivity  |
| $\nu$         | kinematic viscosity of air ( $\text{m}^2 \text{ s}^{-1}$ )                          |
| $\in$         | predefined error value  |

## Dimensionless terms

|          |  |
|----------|--|
| $LAI$    | leaf area index  |
| $SF$     | shading factor   |
| $C_d$    | discharge coefficient  |
| $C_{rs}$ | wind coefficient   |
| $Nu$     | Nusselts number [ $h d_{ci}/\mu_{fa}$ ]                      |
| $Pr$     | Prandtl number [ $c_{p\mu_{fa}}/k_{fa}$ ]                    |
| $Gr$     | Grashof number [ $g\Lambda_{fa}(T_{ab} - T_{fa})d^3/\nu^3$ ] |
| $Ra$     | Rayleigh number [ $GrPr$ ]                                   |

## References

- Abdel-Ghany, A. M., E. Goto, and T. Kozai. 2006. Evaporation characteristics in a naturally ventilated, fog-cooled greenhouse. *Renewable Energy*, 31(14): 2207–2226.
- Al-Helal, I., N. Al-Abbadi, and A. Al-Ibrahim. 2006. A study of evaporative cooling pad performance for a photovoltaic powered greenhouse. *Acta Horticulturae*, 710: 153–164.
- Ali, B. 2017. Techno-economic optimization for the design of solar chimney power plants. *Energy Conversion and Management*, 138: 461–473.
- Al-Kayiem, H. H., and O. C. Aja. 2016. Historic and recent progress in solar chimney power plant enhancing technologies. *Renewable and Sustainable Energy Reviews*, 58: 1269–1292.
- Andersen, K. T. 1995. Theoretical considerations on natural ventilation by thermal buoyancy. *ASHRAE Transactions*, 101(2): 1103–1117.
- Arbel, A., O. Yekutieli, and M. Barak. 1999. Performance of a fog system for cooling greenhouses. *Journal of Agricultural Engineering Research*, 72(2): 129–136.
- Bansal, N. K., J. Mathur, S. Mathur, and M. Jain. 2005. Modeling of window-sized solar chimneys for ventilation. *Building and Environment*, 40(10): 1302–1308.
- Bartzanas, T., and C. Kittas. 2005. Heat and mass transfer in a large evaporative cooled greenhouse equipped with a progressive shading. *Acta Horticulture*, 691: 625–632.
- Bassiouny, R., and N. S. A. Koura. 2008. An analytical and numerical study of solar chimney use for room natural ventilation. *Energy Buildings*, 40(5): 865–873.
- Bello, R. S., C. N. Ezebuilo, K. A. Eke, and T. A. Adegbulugbe. 2015. Performance characteristics of modelled tri-wing solar chimney and adaptation to wood drying. In *Solar Radiation Applications*, ed. R. S. Bello, ch. 3, 53–71. InTech.
- Boulard, T., and A. Baille. 1993. A simple greenhouse climate control model incorporating effects of ventilation and evaporative cooling. *Agricultural and Forest Meteorology*, 65(3-4): 145–157.
- Boulard, T., R. Haxaire, M. A. Lamrani, J. C. Roy, and A. Jaffrin. 1999. Characterization and modeling of the air fluxes induced by natural ventilation in a greenhouse. *Journal of Agricultural Engineering Research*, 74(2): 135–144.
- Bréda, N. J. J. 2003. Ground-based measurements of leaf area index: a review of methods, instruments and current controversies. *Journal of Experimental Botany*, 54(392): 2403–2417.
- Burek, S. A. M., and A. Habeb. 2007. Air flow and thermal efficiency characteristics in solar chimneys and Trombe Walls. *Energy and Buildings*, 39(2): 128–135.
- F-Chart Software. 2002. Available at: <http://www.fchart.com/ees/>. Accessed 5 Jan 2017.
- Ganguly, A., D. Misra, and S. Ghosh. 2010. Modeling and analysis of solar photovoltaic-electrolyzer-fuel cell hybrid power system integrated with floriculture greenhouse. *Energy and Buildings*, 42(11): 2036–2043.
- Ganguly, A., and S. Ghosh. 2007. Modeling and analysis of a fan-pad ventilated floricultural Greenhouse. *Energy and Buildings*, 39(10): 1092–1097.
- Ganguly, A., and S. Ghosh. 2009. Model development and experimental validation of a floriculture greenhouse under natural ventilation. *Energy and Buildings*, 41(5): 521–527.
- Incropera, F. P., and D. P. Dewitt. 2006. *Fundamental of Heat and Mass Transfer*. 6th ed. New Jersey: JohnWiley and Sons.
- Kittas, C., T. Boulard, and G. Papadakis. 1997. Natural ventilation of a greenhouse with ridge and side openings: sensitivity to temperature and wind effects. *Transactions of ASAE*, 40(2): 415–425.
- Koonsrisuk, A., and T. Chitsomboon. 2013. Mathematical modeling of solar chimney power plants. *Energy*, 51: 314–322.
- Mathur, J., N. K. Bansal, S. Mathur, and M. Jain. 2006. Experimental investigations on solar chimney for room ventilation. *Solar Energy*, 80(8): 927–935.
- Mirja, A. S., Misra, D., and S. Ghosh. 2016. Study the performance of a fogging system for a naturally ventilated, fog-cooled greenhouse. *Journal of Energy Research and Environmental Technology*, 3(1): 19–23.
- Misra, D., and S. Ghosh. 2013. Thermal modeling of a ridge-ventilated greenhouse equipped with longitudinally distributed evaporative cooling pads. *International Journal of*

- Emerging Technology and Advanced Engineering*, 3(Special Issue 3): 348–355.
- Misra, D., and S. Ghosh. 2017a. Performance study of a floricultural greenhouse surrounded by shallow water ponds. *International Journal of Renewable Energy Development*, 6(2): 137–144.
- Misra, D., and S. Ghosh. 2017b. Microclimatic modeling and analysis of a fog-cooled naturally ventilated greenhouse. *International Journal of Environment, Agriculture and Biotechnology*, 2(2): 997–1002.
- Ong, K. S. 2003. A mathematical model of a solar chimney. *Renewable Energy*, 28(7): 1047–1060.
- Ong, K. S., and C. C. Chow. 2003. Performance of a solar chimney. *Solar Energy*, 74(1): 1–17.
- Panse, S. V., A. S. Jadhav, A. S. Gudekar, and J. B. Joshi. 2011. Inclined solar chimney for power production. *Energy Conversion and Management*, 52(10): 3096–3102.
- Rachmat, R., and K. Horibe. 1999. Solar heat collection characteristics of a fiber reinforced plastic drying house. *Transactions of the ASAE*, 42(1): 149–157.
- Saleem, A. A., M. Bady, S. Ookawara, and A. K. Abdel-Rahman. 2016. Achieving standard natural ventilation rate of dwellings in a hot-arid climate using solar chimney. *Energy and Buildings*, 133: 360–370.
- Sampson, D. A., and H. L. Allen. 1995. Direct and indirect estimates of leaf area index (LAI) for lodgepole and loblolly pine stands. *Trees*, 9(3): 119–122.
- Smolík, J., L. Džumbová, J. Schwarz, and M. Kulmala. 2001. Evaporation of ventilated water droplet: connection between heat and mass transfer. *Journal of Aerosol Science*, 32(6): 739–748.
- Swinbank, W. C. 1963. Long-wave radiation from clear skies. *Quarterly Journal of the Royal Meteorological Society*, 89(381): 339–348.
- Tan, A. Y. K., and N. H. Wong. 2013. Parameterization studies of solar chimneys in the tropics. *Energies*, 6(1): 145–163.
- Teitel, M., and J. Tanny. 1999. Natural ventilation of greenhouses: experiments and model. *Agricultural and Forest Meteorology*, 96(1–3): 59–70.
- Tiwari, G. N. 2002. *Solar Energy-Fundamentals, Design, Modeling and Applications*. New Delhi, India: Narosa Publishing House.
- Zaragozaa, G., M. Buchholzb, P. Jochumb, and J. Pérez-Parra. 2007. Watergy project: Towards a rational use of water in greenhouse agriculture and sustainable architecture. *Desalination*, 211(1-3): 296–303.